

UC Berkeley

UC Berkeley Previously Published Works

Title

Aurora Kinase A inhibition enhances DNA damage and tumor cell death with 131I-MIBG therapy in high-risk neuroblastoma

Permalink

<https://escholarship.org/uc/item/4fv2q3qt>

Journal

EJNMMI Research, 14(1)

ISSN

2191-219X

Authors

Kumar, Perna

Koach, Jessica

Nekritz, Erin

et al.

Publication Date

2024

DOI

10.1186/s13550-024-01112-7

Peer reviewed

ORIGINAL RESEARCH

Open Access



Aurora Kinase A inhibition enhances DNA damage and tumor cell death with ^{131}I -MIBG therapy in high-risk neuroblastoma

Perna Kumar^{1,2*†}, Jessica Koach^{2†}, Erin Nekritz², Sucheta Mukherjee², Benjamin S. Braun^{2,7}, Steven G. DuBois³, Nicole Nasholm², Daphne Haas-Kogan⁴, Katherine K. Matthay^{2,7}, William A. Weiss^{2,5,7}, Clay Gustafson^{2,7†} and Youngho Seo^{6,7†}

Abstract

Background Neuroblastoma is the most common extra-cranial pediatric solid tumor. ^{131}I -metaiodobenzylguanidine (MIBG) is a targeted radiopharmaceutical highly specific for neuroblastoma tumors, providing potent radiotherapy to widely metastatic disease. Aurora kinase A (AURKA) plays a role in mitosis and stabilization of the MYCN protein in neuroblastoma. We aimed to study the impact of AURKA inhibitors on DNA damage and tumor cell death in combination with ^{131}I -MIBG therapy in a pre-clinical model of high-risk neuroblastoma.

Results Using an in vivo model of high-risk neuroblastoma, we demonstrated a marked combinatorial effect of ^{131}I -MIBG and alisertib on tumor growth. In *MYCN* amplified cell lines, the combination of radiation and an AURKA A inhibitor increased DNA damage and apoptosis and decreased MYCN protein levels.

Conclusion The combination of AURKA inhibition with ^{131}I -MIBG treatment is active in resistant neuroblastoma models.

Keywords Neuroblastoma, Aurora Kinase A inhibitors, ^{131}I -MIBG, Metaiodobenzylguanidine, Radiopharmaceutical

[†]Perna Kumar and Jessica Koach these authors are co-first authors.

[†]Clay Gustafson and Youngho Seo these authors are Co-senior authors.

*Correspondence:

Perna Kumar
perna@uic.edu

¹ Department of Pediatrics, University of Illinois College of Medicine at Peoria, 530 NE Glen Oak Ave, Peoria, IL 61637, USA

² Department of Pediatrics, University of California, San Francisco, CA, USA

³ Dana-Farber/Boston Children's Cancer and Blood Disorders Center, Harvard Medical School, Boston, MA, USA

⁴ Department of Radiation Oncology, Dana-Farber Cancer Institute, Brigham and Women's Hospital, Harvard Medical School, Boston, MA, USA

⁵ Departments of Neurology, Neurosurgery, and Brain Tumor Research Center, University of California San Francisco, San Francisco, CA, USA

⁶ Department of Radiology and Biomedical Imaging, University of California, San Francisco, CA, USA

⁷ Helen Diller Family Comprehensive Cancer Center, UCSF, San Francisco, CA, USA

Introduction

Neuroblastoma, a tumor of the sympathetic nervous system, is the most common extra-cranial pediatric solid tumor. High-risk disease accounts for approximately half of all initial presentations and 15% of pediatric cancer related mortality [1]. Neuroblastoma has two unique vulnerabilities—selective uptake of metaiodobenzylguanidine (MIBG) and frequent amplification of the *MYCN* oncogene.

Neuroblastoma is a radio-sensitive tumor which is why external beam radiation is a critical part of the current standard of care [2]. MIBG is a norepinephrine analog that, when radiolabeled with I-131, provides selective radiation therapy via uptake by the human norepinephrine transporter (hNET), which is widely expressed on the neuroblastoma cell surface [3]. ^{131}I -MIBG is an active agent used to treat relapsed and refractory

neuroblastoma and is currently being studied in newly diagnosed patients with high-risk disease in a randomized Phase 3 trial (NCT03126916) and as Phase 2 induction therapy [4]. MIBG has a reported response rate of 25–40% in relapsed and refractory disease [5, 6].

MYCN is a transcription factor oncogene and known driver of neuroblastoma associated with high-risk disease and poor overall survival. As such, *MYCN* is a tempting therapeutic target; however, directly inhibiting *MYCN* is challenging since it is not an easily druggable enzyme. In addition, as a transcription factor important in cell division, *MYCN* has a broad impact on both healthy and malignant cell function. Aurora kinase A (AURKA) stabilizes *MYCN* through a scaffolding function independent of its kinase activity and protects it from proteolytic degradation [7]. It has been shown that AURKA inhibitors disrupt the Aurora-A/*MYCN* complex, triggering proteasomal degradation and resulting in decreased expression of *MYCN* protein, regression of tumors, and extended survival in mouse models [7–9].

We aimed to study the impact of AURKA inhibitors on DNA damage and tumor cell death when given in combination with ^{131}I -MIBG therapy in high-risk neuroblastoma.

Background

Aurora kinase inhibitors

Aurora kinase inhibitors have demonstrated radio-sensitization in hepatocellular carcinoma where combination therapy with VE-465 and external beam radiation interrupted the cell cycle *in vitro* and significantly enhanced radiation-induced death *in vivo* [10].

Alisertib, a competitive reversible AURKA inhibitor, directly blocks kinase activity and disrupts the assembly of mitotic spindles, the segregation of chromosomes, and the proliferation of cells by regulating entry into mitosis [11–15]. Increased expression of AURKA, independent of *MYCN* amplification, is a negative prognostic factor in neuroblastoma, and AURKA inhibition with alisertib has shown efficacy in pre-clinical cell line xenograft models [16, 17] as well as activity and safety in a pediatric Phase I trial in combination with chemotherapy [18]. Recent investigations into the role of AURKA inhibitors in the DNA damage response pathway and DNA repair have identified additional mechanisms by which AURKA inhibitors may be a promising cancer therapy [19–21].

AURKA inhibition using LY compounds has shown anti-tumor activity in pre-clinical studies [22] which has led to further investigation for a variety of solid tumors including advanced EGFR mutant non-squamous lung cancer (NCT05017025), small cell lung cancer (NCT03898791), metastatic breast cancer (NCT03955939), and relapsed/refractory neuroblastoma

(NCT04106219). A phase I clinical trial studying erubromine (LY3295668) in patients with locally advanced or metastatic solid tumors showed that the drug was well tolerated overall with stable disease for nine of thirteen enrolled patients (disease control rate of 69%) [23].

Combination therapies with ^{131}I -MIBG

We have previously investigated the radio-sensitizing effect of vorinostat, a histone deacetylase (HDAC) inhibitor, in neuroblastoma. When treated with external beam radiation and drug, tumor cells showed increased cell death *in vitro* and decreased tumor growth *in vivo* [24]. Vorinostat treated tumors showed reduced levels of Ku-86, a DNA repair enzyme, that potentiates the effect of radiation in cultured neuroblastoma cells [24]. Vorinostat treatment also increases the expression of hNET, the main transporter of MIBG, in neuroblastoma cells [25]. Subsequent clinical trials combining vorinostat and ^{131}I -MIBG, showed combinatorial efficacy with improved responses compared to MIBG alone [26]. This successful translation of a targeted therapy in combination with ^{131}I -MIBG from pre-clinical models to clinical trials is encouraging for the development of additional synergistic agents to further improve response rates.

Study of MIBG *in vivo* using mouse models

Though MIBG has been studied *in vivo* using a variety of neuroblastoma and pheochromocytoma mouse models, most of these transgenic and xenograft neuroblastoma models are MIBG non-avid, possibly through loss of hNET. Only a few *in vivo* studies showing MIBG uptake have been published, including an SK-N-SH line where pinhole imaging of xenograft tumors with ^{131}I -MIBG was possible [27] and a study of ultratrace MIBG in a SK-N-BE(2c) model [28]. Our current NB1691-LUC/NET mouse model is among the only published high-risk neuroblastoma mouse models which takes up and retains significant and reproducible amounts of MIBG [29]. Using lentiviral transduction to exogenously express the hNET receptor in a luciferase labeled neuroblastoma cell line [30], we show that the NB1691-LUC/NET model is MIBG avid, *MYCN* amplified, and radio-resistant, and provides easy tracking of disease with bioluminescence.

Materials and methods

Please see supplemental data (Additional file 1) for more detailed descriptions of the materials and methods, which have been condensed for simplicity and included here.

Cell culture

SK-N-BE(2), Kelly, and NB1691-Luc cell lines were transduced to over express hNET as described above to

enhance MIBG uptake [26]. All neuroblastoma cells were grown in DMEM media with 10% FBS, except for Kelly cells, which were grown in RPMI media with 10% FBS. Cells were maintained at 37 °C in humid air with 5% CO₂.

Cell viability assay

Neuroblastoma cells were pre-seeded into 96-well plates for 24 h prior to alisertib and LY3295668 treatment for 4 h followed by external beam radiation. Cell viability was measured 72 h post treatment using CellTiter-Glo assay. Luminescence was read on the Synergy Neo2 microplate reader.

Immunofluorescence

Cells were pre-seeded on glass coverslips in 6-well plates. 24 h post seeding, cells were treated with various concentrations of alisertib for either 24 h (for G2/M cell cycle arrest) or for 4 h followed by external beam radiation (for DNA damage analysis). Nocodazole was used as positive control to arrest cells in G2/M. Cells were fixed then permeabilized. Goat serum was used to block the cells before overnight incubation with primary antibodies. Cells were incubated with secondary antibody then mounted onto glass slides with mounting medium containing Dapi. Slides were imaged on the Leica DMi8 fluorescence microscope. Quantification of arrested cells and the number of DNA damage foci markers were performed using Fiji Image J software.

Western blotting

Cells were lysed with RIPA lysis buffer. Western blots were performed using standard protocol.

Flow cytometry

Kelly, SK-N-BE(2) and NB1691-LUC cells were pre-seeded in 6-well plates for 24 h prior to alisertib treatment.

Cell cycle arrest analysis

Cells were treated with alisertib for 4 and 24 h then harvested and washed. Cells were fixed and permeabilized. Cells were stained with DAPI and analyzed with the BD LSR II flow cytometer. Analysis was performed using Cytobank software.

Cell apoptosis analysis

Cells were treated with alisertib for 4 h followed by external beam radiation. Cells were harvested 48 and 72 h post treatment and washed and stained. Flow cytometry was performed and data was analyzed using FlowJo software.

Immunohistochemistry

Xenograft neuroblastoma tumors, treated with alisertib and MIBG, were excised from mice and paraffin fixed for

Hematoxylin and Eosin staining and analysis of cleaved caspase-3 expression using standard immunohistochemistry protocols.

In vitro radiation

Radiation was administered via a Cesium-137 irradiator. Cells were irradiated for 1.4 min to receive 4 Gy.

In vivo studies

NOD SCID gamma mice were implanted with NB1691-LUC/NET neuroblastoma cells [29]. Tumor bearing mice were treated with alisertib or saline control for 7 days via intraperitoneal (IP) injection. IP injection, which has been used previously [31, 32], was used to minimize the radiation exposure of the handler while dosing. The combination and MIBG cohorts received 37 MBq (1 mCi) of ¹³¹I-MIBG 24 h after the first dose of alisertib or alisertib carrier for the MIBG alone arm. Tumor size was assessed twice weekly for 25 days. Mice were euthanized once maximum tumor length reached 2.0 cm in long axis. Tumor growth was analyzed by a linear mixed effects model, similar to that described by Akutagawa et al. [33]. Tumor volume, as calculated from caliper measurements, was transformed by square root to correct for heteroscedasticity and normalize residuals. Fixed effects included assigned treatment and time. Random effects were included for individual mice. Confidence intervals were estimated by the bootstrap method at the 95% level. All experiments on live vertebrates were performed in accordance with relevant institutional and national guidelines and approved by the UCSF Animal Care and Use Committee (IACUC).

Results

¹³¹I-MIBG dosimetry: Identifying the ideal dose of ¹³¹I-MIBG for combination therapy

To understand the estimated radiation dose from ¹³¹I-MIBG, prior studies were completed using ¹²⁴I-MIBG as a quantitative tool for tumor imaging and dosimetry in vivo [29]. Several studies have estimated human-equivalent internal radiation doses using ¹²⁴I-MIBG and PET/CT in murine NB1691-LUC/NET xenograft models [29, 34]. From those prior results, it was estimated that administration of 52.8–206 MBq (1.43–5.57 mCi) ¹³¹I-MIBG delivers approximately 20 Gy radiation directly to the tumor. In other words, the estimated absorbed dose in tumors was 0.234 Gy/MBq.

Using the NB1691-LUC/NET model [29], we first performed an ¹³¹I-MIBG dose finding experiment to determine the optimal dose for a response to ¹³¹I-MIBG monotherapy (Fig. 1A). Treatment of NB1691-LUC/NET mouse tumors with ¹³¹I-MIBG alone showed decreased tumor growth for mice treated with 74 MBq (2 mCi

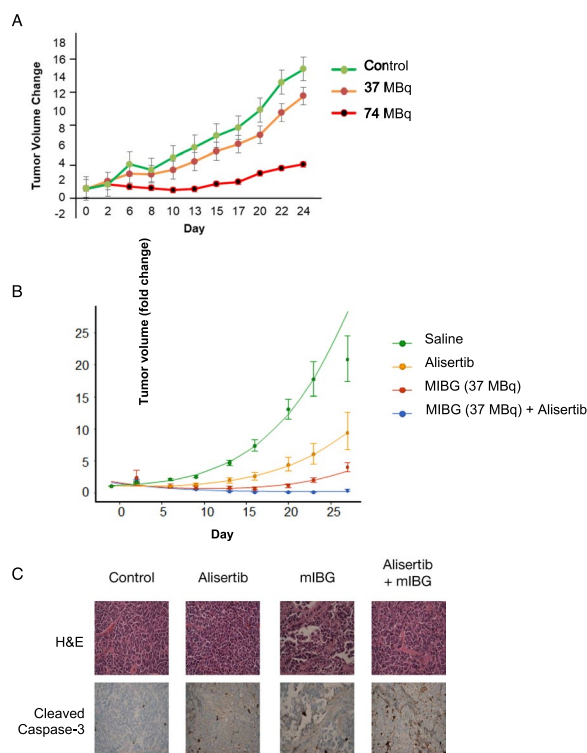


Fig. 1 Alisertib and MIBG treatment decreases neuroblastoma tumor growth. **A** Identifying the ideal dose of ^{131}I -MIBG for combination therapy. Mice were treated with control sham, 37 MBq, or 74 MBq. **B** Alisertib and ^{131}I -MIBG inhibited tumor growth and increased response to ^{131}I -MIBG in NB1691-LUC/NET xenograft mice ($n = 5$ per arm). **C** Immunohistochemistry analysis showed increased cleaved caspase-3 with combination therapy. Alisertib + MIBG vs MIBG: $p = 0.000216$; Alisertib + MIBG vs Alisertib alone: $p = 1.19 \times 10^{-5}$

dose), marginal therapeutic effect for mice treated with 37 MBq (1 mCi dose), and continuous tumor growth for mice with sham (saline) treatment. Overall, mice tolerated 37 MBq doses safely with good radiation induced effects on tumor growth and little systemic toxicity. We therefore chose 37 MBq for combination therapy to ensure that tumor size differences would remain evaluable with ^{131}I -MIBG in combination with radiosensitizer.

Treatment with alisertib and ^{131}I -MIBG results significantly improved response to ^{131}I -MIBG in vivo

Tumor bearing animals treated with 37 MBq (1 mCi) of ^{131}I -MIBG showed a significant slowing in tumor growth as did tumors treated with alisertib alone, however the combination of alisertib and ^{131}I -MIBG showed not only diminished growth, but a reduction in tumor size and an enhanced response to combination therapy (Fig. 1B). Immunohistochemistry was performed which showed an increase in cleaved caspase-3 with the combination indicating an increase in apoptosis and increased cell death

(Fig. 1C). Mice in all cohorts tolerated therapy without significant toxicity as evaluated by weight and general well-being.

Combination therapy with an AURKA inhibitor and radiation induces increased DNA damage

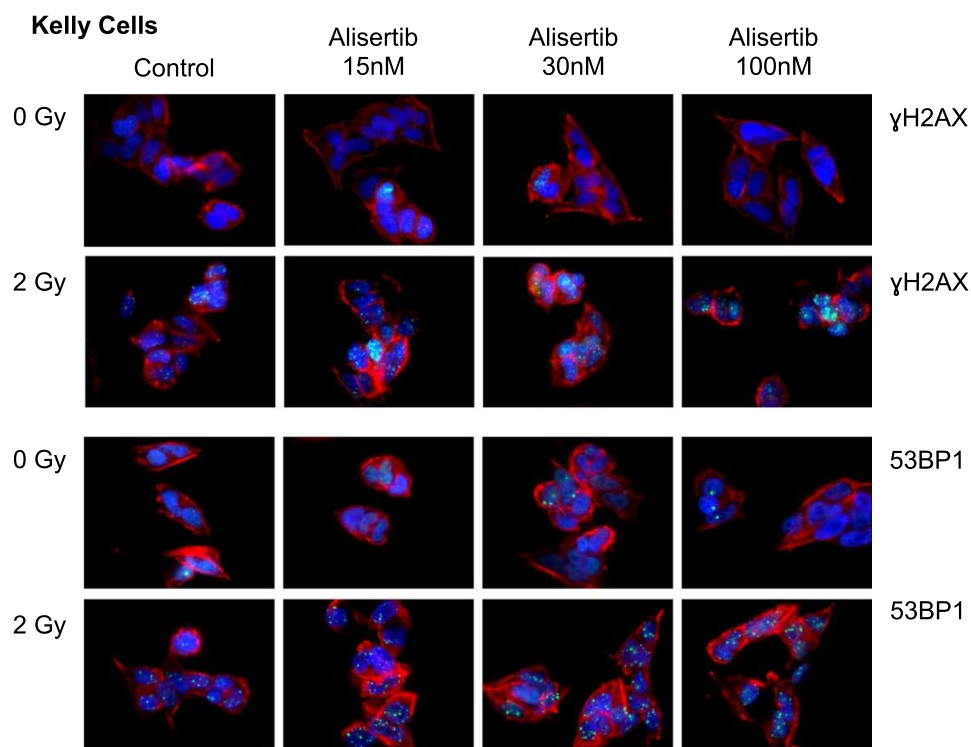
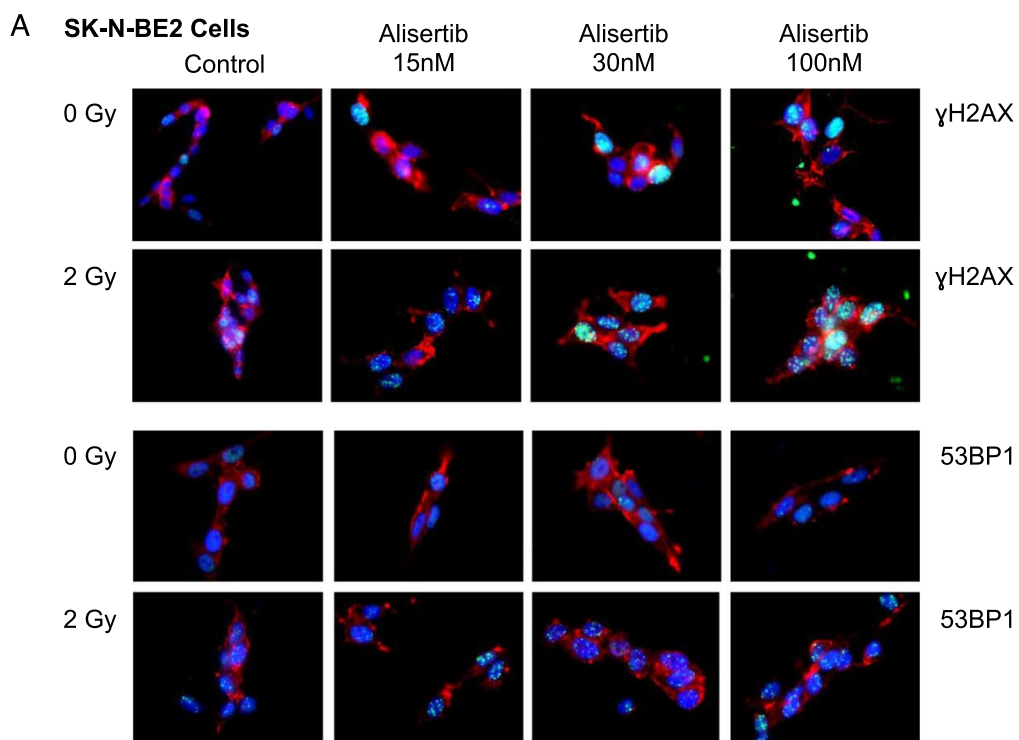
Radiation induces double-stranded breaks (DSBs) in DNA which are marked by phosphorylation of the histone subtype H2AX to recruit DNA repair machinery including the p53BP1 adaptor protein. When cells are exposed to ionizing radiation or DNA-damaging agents, DSBs are generated. An early cellular response to DSBs is the rapid phosphorylation of H2AX at Ser 139 (also known as γ -H2AX). 53BP1 protein is involved in DNA-damage-checkpoint signal transduction and localizes to the sites of DNA damage after ionizing radiation. Immunofluorescence of both pH2AX and p53BP1 foci are therefore used to measure the extent of DNA damage from ionizing radiation. There is a clear increase in both pH2AX and p53BP1 foci for cells treated with 30 nM alisertib and 4 Gy radiation compared to control (Fig. 2A). A dose response with alisertib alone and in combination with radiation shows a clear, dose dependent, and statistically significant increase in DNA damage in the combination compared with pre-treatment with alisertib alone (Fig. 2B).

Combination therapy with AURKA inhibitors followed by external beam radiation drives tumor cell death as measured by apoptosis

We tested alisertib combined with external beam radiation on neuroblastoma cells derived from high-risk patients as a surrogate for MIBG therapy. Dose response testing of alisertib with and without radiation showed a leftward shift in the dose response curve indicating increased potency of the combination, manifesting as a significant decrease in the EC_{50} for alisertib (Fig. 3A). A significant increase in apoptosis was observed in the SK-N-BE2 and Kelly cell lines, though this was not as notable in the NB1691 cell line (Fig. 3B). Dose response testing of LY3295668 with and without radiation also showed a leftward shift in the dose response curve, indicating increased potency of the combination, manifesting as a significant decrease in the EC_{50} for LY3295668 (Fig. 4A). Increased N-myc degradation was observed across all three cell lines and this was dose-dependent (Fig. 4B).

Alisertib arrests neuroblastoma cells in G2/M

AURKA plays a prominent role in the cell cycle with known potent effects on cell division, particularly in G2/M transition. The effects of single agent alisertib treatment on mitosis was evaluated by flow cytometry



Dapi (blue), Phalloidin (red), γ H2AX or 53BP1 (green)

Fig. 2 Alisertib and radiation potently increases DNA damage in neuroblastoma cells. **A** Cells treated with increasing doses of alisertib followed by radiation showed increased DNA damage as detected using immunofluorescence staining for γ H2AX and 53BP1 foci. **B** Quantitation of γ H2AX and 53BP1 foci after combination treatment shows significantly greater DNA damage as exhibited by higher numbers of γ H2AX and 53BP1 foci per cell across all cell lines. Blue = DAPI, green = γ H2AX or 53BP1, red = Phalloidin

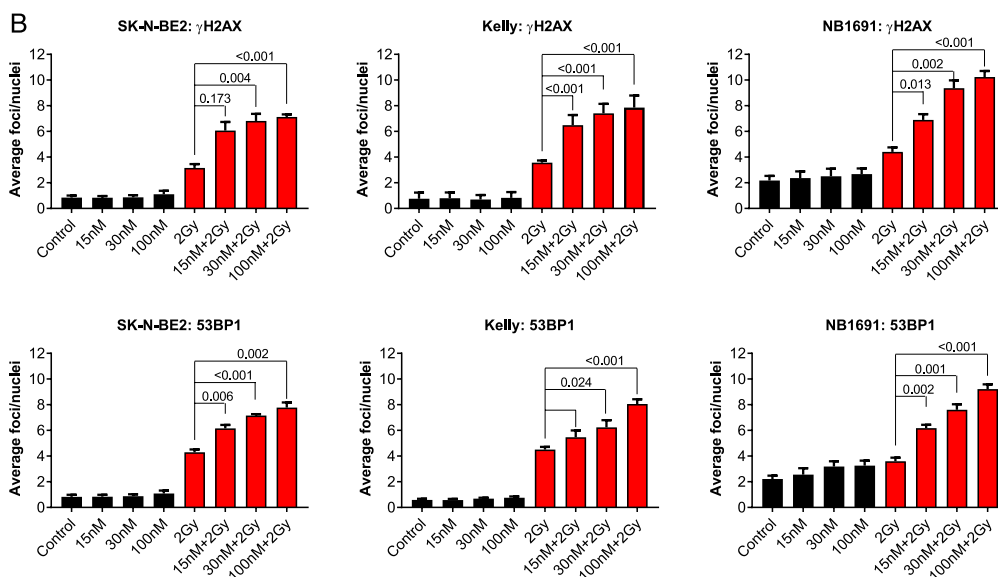
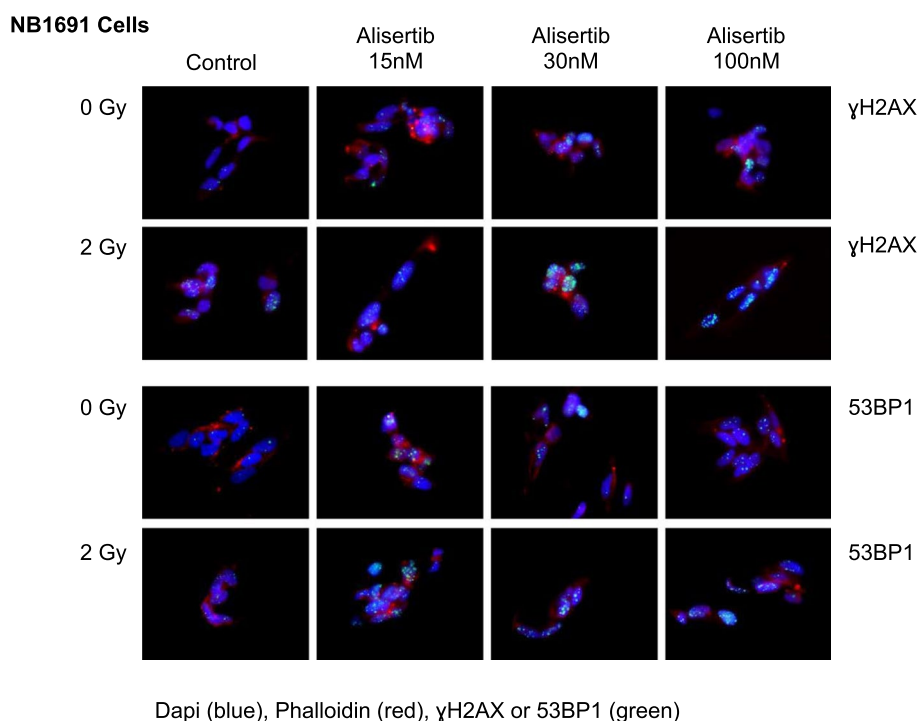


Fig. 2 continued

(Fig. 5A) and immunofluorescence (Fig. 5B). Alisertib treatment showed prominent G2/M arrest starting within 4 h of treatment and eventually mitotic catastrophe resulting in uni- or multi-polar spindle formation. Combination treatment with alisertib and external beam radiation led to a decrease in mitotic cells, potentially during DNA repair; alisertib-induced G2/M arrest was not affected by radiation (Fig. 5C).

We hypothesized that the mechanism of combinatorial efficacy for AURKA inhibitors plus radiation or ¹³¹I-MIBG in neuroblastoma is through cell cycle arrest in G2/M, potentially allowing for open decondensed chromatin, exposing DNA to additional radiation damage and eventually leading to increased cell death by apoptosis.

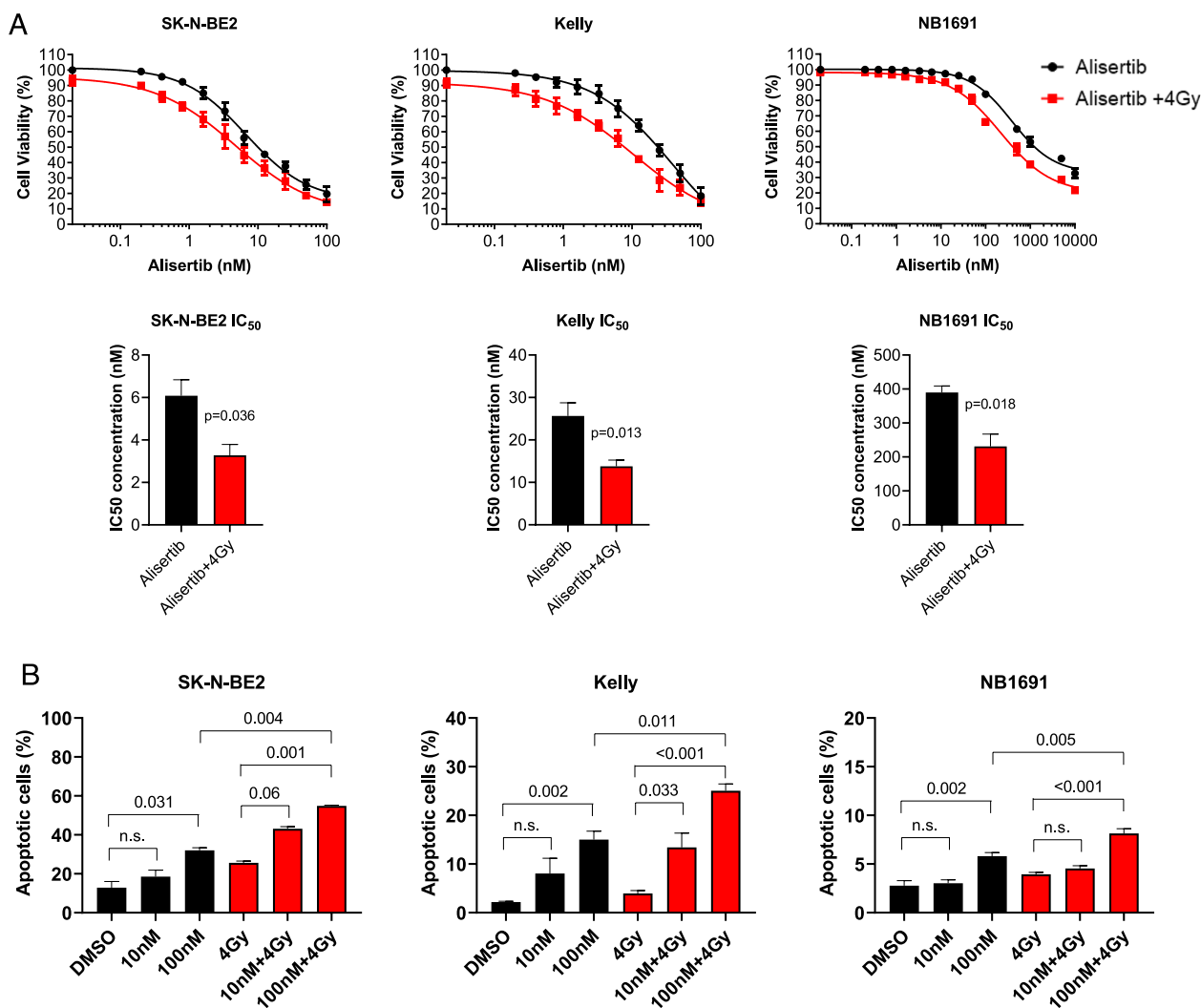


Fig. 3 Treatment with alisertib and radiation in neuroblastoma cell lines induces cell death. **A** Dose response of alisertib with and without radiation across three MYCN amplified cell lines pre-treated with alisertib followed by radiation showed a lower IC50 concentration; SK-N-BE(2) ($p=0.036$); Kelly ($p=0.013$); NB1691-LUC ($p=0.018$) ($n=8$ per arm). Data for IC50 concentrations were normalized to account for the effect from radiation alone. **B** Flow cytometry analysis showed a significant increase in apoptosis with alisertib treatment followed by radiation

Combination radiation and alisertib therapy induces apoptosis and checkpoint control pathways

To better understand the mechanism of action behind the effects of combination therapy, we treated cells with alisertib 4 h prior to 4 Gy radiation and harvested cells at 24 and 48 h. The subsequent western blot reveals marked changes in the checkpoint kinase pathways as well as apoptosis depending on the drug tested. Alisertib shows on-target activity by decreasing AURKA auto-phosphorylation as well as by blocking Histone H3 phosphorylation across all cell lines (Fig. 6). Alisertib also downregulates MYCN protein at 24 h and shows induction of apoptotic markers cleaved PARP and cleaved caspase-3. The induction of apoptosis is notably enhanced

when alisertib is combined with radiation, as measured by cleaved PARP and cleaved caspase-3. Further, radiation combined with alisertib induces sustained phosphorylation of Chk2 (a marker of ongoing DNA repair) for at least 48 h and induces increased phosphorylation of H2AX (a marker of DNA damage) by western blot which is consistent with the immunofluorescence data in Fig. 2.

Discussion

Patients with high-risk neuroblastoma and MYCN amplification have approximately a 40–50% overall survival, despite intensive multi-modal therapies. Thus, novel radio-sensitizing therapies are critical to improving outcomes in this patient population. Dosing, timing,

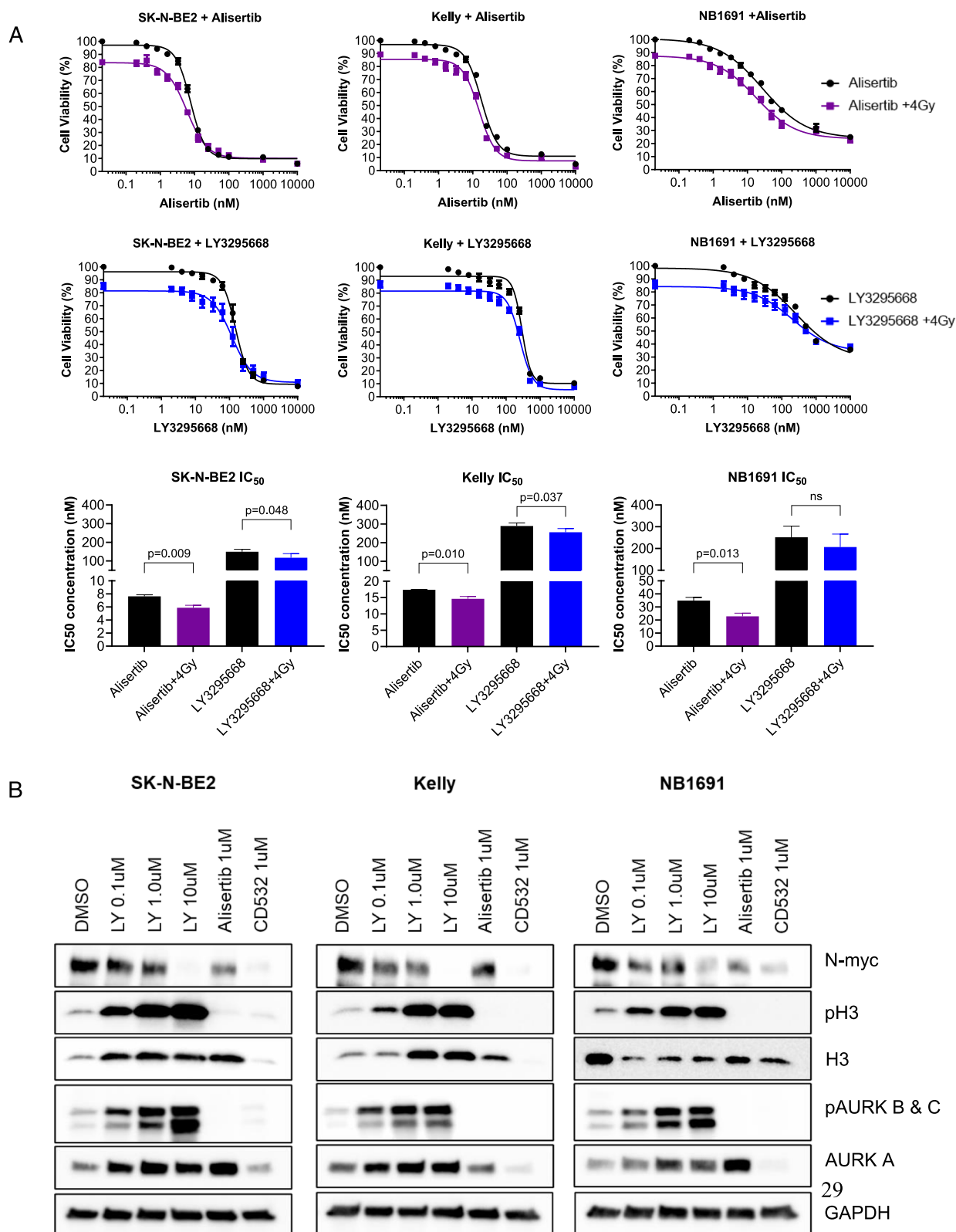


Fig. 4 Treatment with LY3295668 and radiation neuroblastoma cell lines induces cell death. **A** Dose response of LY3295668 with and without radiation across three MYCN amplified cell lines pre-treated with LY3295668 followed by radiation showed a lower IC₅₀ concentration. Data for IC₅₀ concentrations were normalized to account for the effect from radiation alone. **B** Immunoblots of cells treated with LY3295668 show that treatment increased N-myc and AURKA degradation in a dose-dependent manner

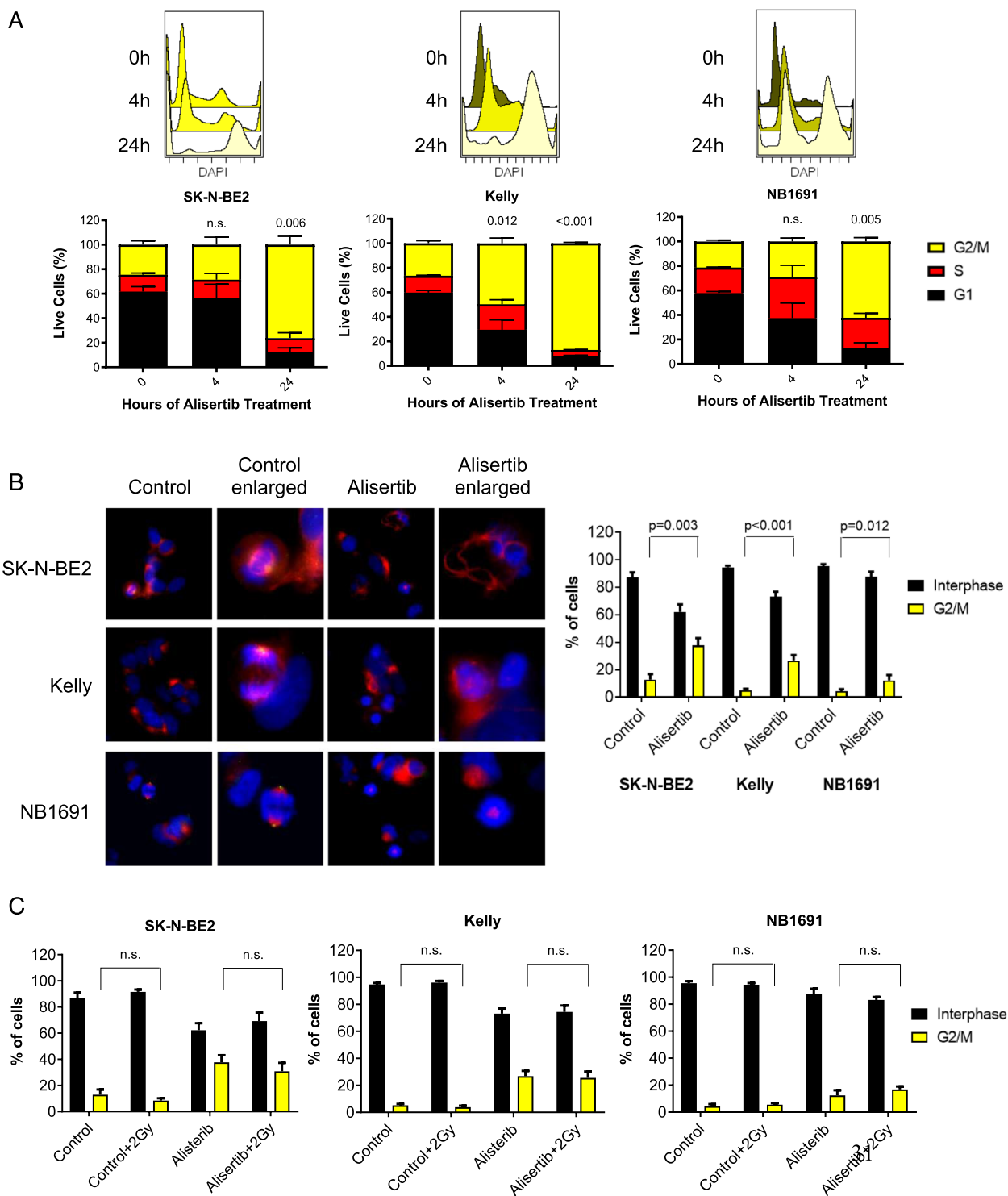


Fig. 5 Alisertib arrests neuroblastoma cells in G2/M. **A** Flow cytometry analysis of neuroblastoma cells treated with alisertib showed significant increases in G2/M cell cycle arrest after 24 h; SK-N-BE(2) ($P=0.006$); Kelly ($P<0.001$); NB1691-LUC ($P=0.005$). **B** Immunofluorescence staining of the nucleus (blue), α -tubulin (red) and pAURKA (green) in cells treated with alisertib demonstrates uni- or multi-polar spindle formations and significant induction of cells to arrest in G2/M phase compared to non-treated cells; SK-N-BE(2) ($P=0.003$); Kelly ($P<0.001$); NB1691-LUC ($P=0.012$). **C** γ -radiation does not impact G2/M cell cycle arrest. Data represent the % of cells arrested in G2/M

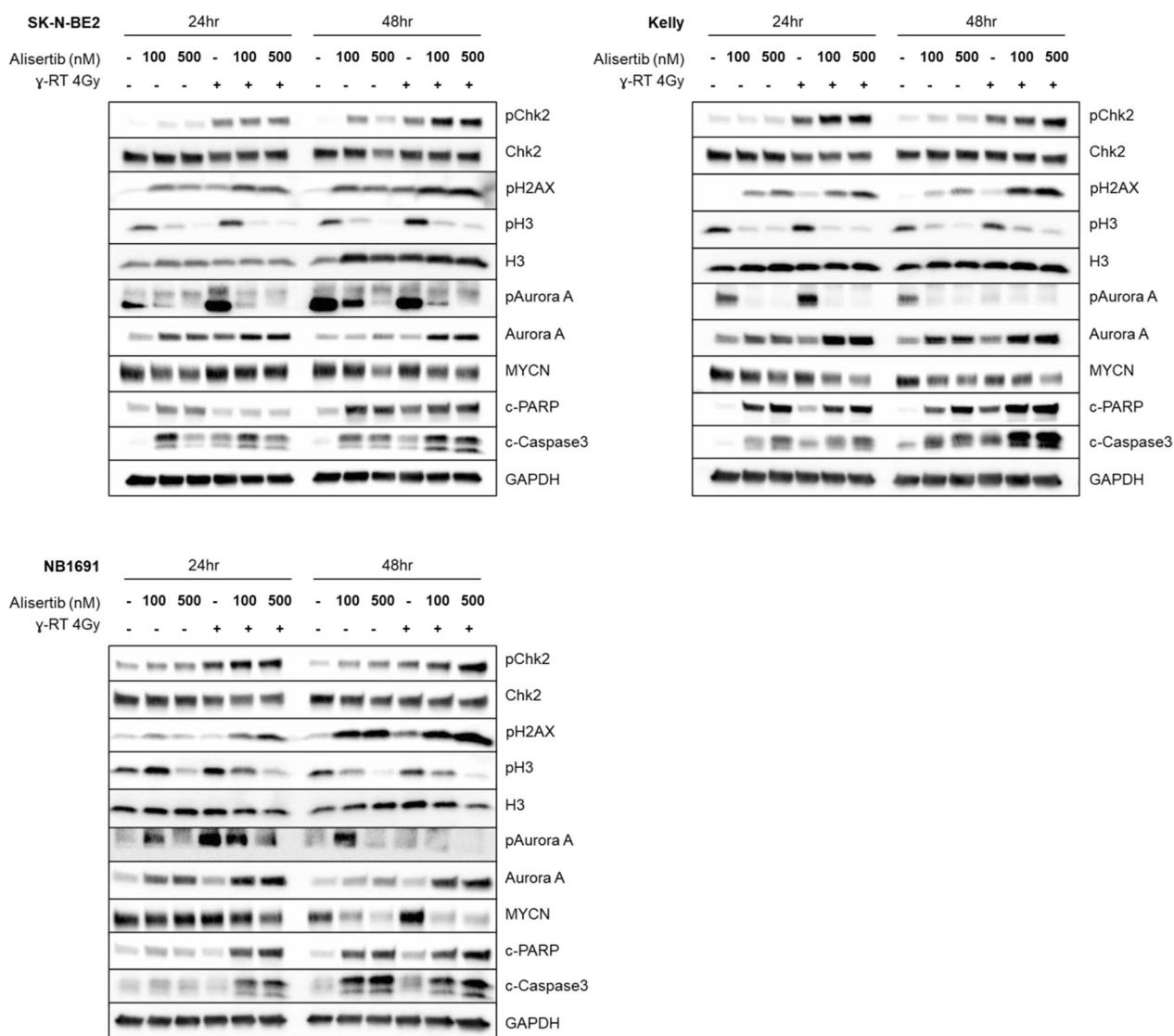


Fig. 6 Alisertib and radiation therapy potently induces apoptosis, downregulates MYCN protein, increases DNA damage, and enhances/prolongs Chk2 activation. Immunoblots of cells treated with alisertib and radiation show that treatment increases and prolongs pChk2 and pH2AX expression, decreases pH3 and pAURKA, and increases cleaved PARP and cleaved caspase-3 expression

and duration of drug therapy and radiation therapy can all impact the radio-sensitization of a given combination, which highlights the importance of in vivo testing prior to advancement to patients in clinical trials. In our study, we showed that combining an AURKA inhibitor with a targeted radiopharmaceutical markedly decreased tumor growth in vivo compared to either agent alone. The mechanism underlying the improved efficacy of the combination of an AURKA inhibitor and radiation or ¹³¹I-MIBG is through loss of AURKA activity and subsequent blockade of cells in G2/M with enhanced DNA damage and loss of MYCN, resulting in increased apoptosis and cell death.

Neuroblastoma is typically highly responsive to radiation which is why external beam radiation to the tumor bed after surgical resection of the primary tumor is a critical component of therapy. Though external beam radiation is effective in eliminating microscopic residual disease and minimizing the risk for relapse, it has several limitations including, most notably, the inability to target widespread metastatic disease or patchy bone marrow involvement, which can be common in refractory disease. ¹³¹I-MIBG, however, allows for targeted delivery of radiation to all sites of MIBG avid disease, and given its prolonged half-life, can do so

for a sustained period of time (unlike external beam radiation which can only be given in limited fractions locally).

Using both a novel mouse model of MIBG avid neuroblastoma and high-risk neuroblastoma cell lines treated with radiation as a surrogate for ^{131}I -MIBG, we showed that alisertib in combination with radiation enhances DNA damage and impairs/prolongs DNA repair, as evidenced by the persistence of pH2AX, a marker of double-stranded DNA breaks. It is likely that destabilization of MYCN is not the only effect of AURKA inhibitors such as alisertib and LY3295668, both from these mechanistic studies and also from a Phase I trial of alisertib combined with chemotherapy in which significant responses occurred in patients whose tumors were MYCN non-amplified [18]. Other studies have suggested that alisertib treatment promotes non-homologous end joining and impairs homologous recombination. In our model systems, this hypothesis is supported by the increase in phosphorylated Chk2 expression which is reported to increase activity of BRCA1 and BRCA2, increase pH2AX, increase DNA-PKcs activity, and induce DNA double-stranded breaks [22, 35]. The *in vitro* activation of checkpoint kinase pathways and cell cycle arrest further suggests that combination therapy halts natural progression through the cell cycle, likely due to checkpoint regulation and the inability of the cell to properly repair damaged DNA.

Limitations of this research include the fixed dosing and schedule of therapy administration *in vivo* as well as the evaluation of mechanism only *in vitro* using MYCN-amplified cell lines. ^{131}I -MIBG is thought to work by accumulating in clusters of neuroblastoma tumor cells and within each neuroblastoma cell serving as a mini-irradiator for its neighboring cells, making *in vivo* experiments reflective of human tumors; however because of the significant logistical barriers to performing molecular testing on live cells in radioactive tumor-bearing mice, we elected to use cell line models of high-risk neuroblastoma to further elucidate the mechanism.

Conclusion

We have demonstrated that AURKA inhibition by alisertib or LY3295668 in combination with selective radiation therapy with ^{131}I -MIBG or radiation is active in high-risk neuroblastoma. Our NB1691-LUC/NET mouse model can be used for pre-clinical testing of new combinations with ^{131}I -MIBG, and also the head-to-head pre-clinical comparison of different targeted therapies with ^{131}I -MIBG to optimize neuroblastoma treatment.

Abbreviations

MIBG ^{131}I -metaiodobenzylguanidine
AURKA Aurora kinase A

hNET Human norepinephrine transporter
HDAC Histone deacetylase
DSBs Double-stranded breaks

Supplementary Information

The online version contains supplementary material available at <https://doi.org/10.1186/s13550-024-01112-7>.

Additional file 1. Supplemental Data.

Acknowledgements

Not applicable.

Author contributions

PK, JK, EN, SM, BSB, SGD, NN, DHK, KKM, WAW, CG, and YS are the authors on this work, have each contributed to the manuscript in significant ways, and have reviewed and agreed upon the manuscript content. KKM, CG, DHK, and SGD conceived of the original study question. PK, JK, EN, SM, NN, and YS contributed to the theory behind experiments, contributed to sample preparation and data collection, and carried out the experiments. BSB verified the correct computational analysis for tumor volume reduction and contributed to the analytical methods. CG, WAW, and KKM supervised the findings of this work and supervised the project as a whole. All authors discussed the results and contributed to the final manuscript. PK wrote the manuscript with support from JK regarding the detailed methods. JK contributed all the final figures and legends which were edited and incorporated by PK. All authors provided critical feedback and helped shape the research, analysis, and manuscript.

Funding

This research was supported by P01CA081403, R01CA154561, U54CA274516, Cookies for Kids, and Alex's Lemonade Stand Foundation. These organizations had no role in the design of the study; collection, analysis, or interpretation of data; or in writing the manuscript.

Availability of data and materials

The datasets used and/or analyzed during the current study are available from the corresponding author on reasonable request.

Declarations

Ethics approval and consent to participate

Not applicable. Of note, all experiments on live vertebrates were performed in accordance with relevant institutional and national guidelines and approved by the UCSF Animal Care and Use Committee (IACUC).

Consent for publication

Not applicable.

Competing interests

The authors declare that they have no competing interests.

Received: 16 January 2024 Accepted: 16 May 2024

Published online: 13 June 2024

References

1. Matthay KK, Maris JM, Schleiermacher G, et al. Neuroblastoma. *Nat Publ Group*. 2016;2:1–22. <https://doi.org/10.1038/nrdp.2016.78>.
2. Haas-Kogan DA, Swift PS, Selch M, et al. Impact of radiotherapy for high-risk neuroblastoma: a Children's Cancer Group study. *Radiat Oncol Biol*. 2003;56(1):28–39. [https://doi.org/10.1016/s0360-3016\(02\)04506-6](https://doi.org/10.1016/s0360-3016(02)04506-6).
3. Dubois SG, Geier E, Batra V, et al. Evaluation of norepinephrine transporter expression and metaiodobenzylguanidine avidity in neuroblastoma: a report from the children's oncology group. *Int J Mol Imaging*. 2012;2012:250834.

4. Kraal KCJM, Tytgat GAM, van Eck-Smit BLF, Kam B, Caron HN, van Noesel M. Upfront treatment of high-risk neuroblastoma with a combination of 131I-MIBG and topotecan. *Pediatr Blood Cancer*. 2015;62(11):1886–91. <https://doi.org/10.1002/psc.25580>.
5. Wilson JS, Gains JE, Moroz V, Wheatley K, Gaze MN. A systematic review of 131I-meta iodobenzylguanidine molecular radiotherapy for neuroblastoma. *Eur J Cancer*. 2014;50(4):801–15. <https://doi.org/10.1016/j.ejca.2013.11.016>.
6. DuBois SG, Matthay KK. 131I-Metaiodobenzylguanidine therapy in children with advanced neuroblastoma. *Q J Nucl Med Mol Imaging*. 2013;57(1):53–65.
7. Richards MW, Burgess SG, Poon E, et al. Structural basis of N-Myc binding by Aurora-A and its destabilization by kinase inhibitors. *Proc Natl Acad Sci USA*. 2016;113(48):13726–31. <https://doi.org/10.1073/pnas.1610626113>.
8. Meyerowitz JG, Chen J, Benes C, et al. Drugging MYCN through an allosteric transition in Aurora. *Kinase A*. 2014;26(3):414–27. <https://doi.org/10.1016/j.ccr.2014.07.015>.
9. Brockmann M, Poon E, Berry T, et al. Small molecule inhibitors of aurora-a induce proteasomal degradation of N-myc in childhood neuroblastoma. *Cancer Cell*. 2013;24(1):75–89. <https://doi.org/10.1016/j.ccr.2013.05.005>.
10. Lin Z-Z, Chou C-H, Cheng A-L, Liu W-L, Chia-Hsien CJ. Radiosensitization by combining an aurora kinase inhibitor with radiotherapy in hepatocellular carcinoma through cell cycle interruption. *Science*. 2014;135(2):492–501. <https://doi.org/10.1002/jic.28682>.
11. Crosio C, Fimia GM, Loury R, et al. Mitotic phosphorylation of histone H3: spatio-temporal regulation by mammalian Aurora kinases. *Mol Cell Biol*. 2002;22(3):874–85.
12. Liu Q, Kaneko S, Yang L, et al. Aurora-A abrogation of p53 DNA binding and transactivation activity by phosphorylation of serine 215. *J Biol Chem*. 2004;279(50):52175–82. <https://doi.org/10.1074/jbc.M406802200>.
13. Ouchi M. BRCA1 phosphorylation by Aurora-A in the regulation of G2 to M transition. *J Biol Chem*. 2004;279(19):19643–8. <https://doi.org/10.1074/jbc.M311780200>.
14. Scrittore L, Hans F, Angelov D, Charra M, Prigent C, Dimitrov S. pEg2 aurora-A kinase, histone H3 phosphorylation, and chromosome assembly in *Xenopus* egg extract. *J Biol Chem*. 2001;276(32):30002–10. <https://doi.org/10.1074/jbc.M102701200>.
15. Zhao B, Smallwood A, Yang J, et al. Modulation of kinase-inhibitor interactions by auxiliary protein binding: crystallography studies on Aurora A interactions with VX-680 and with TPX2. *Protein Sci*. 2008;17(10):1791–7. <https://doi.org/10.1110/ps.036590.108>.
16. Maris JM, Morton CL, Gorlick R, et al. Initial testing of the aurora kinase A inhibitor MLN8237 by the pediatric preclinical testing program (PPTP). *Pediatr Blood Cancer*. 2010;55(1):26–34. <https://doi.org/10.1002/psc.22430>.
17. Shang X, Burlingame SM, Okcu MF, et al. Aurora A is a negative prognostic factor and a new therapeutic target in human neuroblastoma. *Mol Cancer Ther*. 2009;8(8):2461–9. <https://doi.org/10.1158/1535-7163.MCT-08-0857>.
18. DuBois SG, Marachelian A, Fox E, et al. Phase I study of the Aurora A kinase inhibitor alisertib in combination with irinotecan and temozolomide for patients with relapsed or refractory neuroblastoma: a NANT (new approaches to neuroblastoma therapy) trial. *J Clin Oncol*. 2016. <https://doi.org/10.1200/JCO.2015.65.4889>.
19. Foy V, Schenk MW, Baker K, et al. Targeting DNA damage in SCLC. *Lung Cancer*. 2017;114:12–22. <https://doi.org/10.1016/j.lungcan.2017.10.006>.
20. Do T-V, Hirst J, Hyter S, Roby KF, Godwin AK. Aurora A kinase regulates non-homologous end-joining and poly(ADP-ribose) polymerase function in ovarian carcinoma cells. *Oncotarget*. 2017;8(31):50376–92. <https://doi.org/10.18632/oncotarget.18970>.
21. Alcaraz-Sanabria A, Nieto-Jiménez C, Corrales-Sánchez V, et al. Synthetic lethality interaction between aurora kinases and CHEK1 inhibitors in ovarian cancer. *Mol Cancer Ther*. 2017;16(11):2552–62. <https://doi.org/10.1158/1535-7163.MCT-17-0223>.
22. Du J, Yan L, Torres R, et al. Aurora A-selective inhibitor LY3295668 leads to dominant mitotic arrest, apoptosis in cancer cells, and shows potent preclinical antitumor efficacy. *Mol Cancer Ther*. 2019;18(12):2207–19.
23. Chu QS, Bouganim N, Fortier C, et al. Aurora kinase A inhibitor, LY3295668 erbumine: a phase 1 monotherapy safety study in patients with locally advanced or metastatic solid tumors. *Invest New Drugs*. 2021;39(4):1001–10.
24. Mueller S, Yang X, Sottero TL, et al. Cooperation of the HDAC inhibitor vorinostat and radiation in metastatic neuroblastoma: efficacy and underlying mechanisms. *Cancer Lett*. 2011;306(2):223–9. <https://doi.org/10.1016/j.canlet.2011.03.010>.
25. More SS, Itsara M, Yang X, et al. Vorinostat increases expression of functional norepinephrine transporter in neuroblastoma in vitro and in vivo model systems. *Clin Cancer Res*. 2011;17(8):2339–49. <https://doi.org/10.1158/1078-0432.CCR-10-2949>.
26. DuBois SG, Granger MM, Groshen S, et al. Randomized phase II Trial of MIBG versus MIBG, vincristine, and irinotecan versus MIBG and vorinostat for patients with relapsed or refractory neuroblastoma: a report from NANT consortium. *J Clin Oncol*. 2021;39(31):3506–14.
27. Accorsi R, Morowitz MJ, Charron M, Maris JM. Pinhole imaging of 131I-metaiodobenzylguanidine (131I-MIBG) in an animal model of neuroblastoma. *Pediatr Radiol*. 2003;33(10):688–92. <https://doi.org/10.1007/s00247-003-1006-6>.
28. Barrett JA, Joyal JL, Hillier SM, et al. Comparison of high-specific-activity ultratracer 123I/131I-MIBG and carrier-added 123I/131I-MIBG on efficacy, pharmacokinetics, and tissue distribution. *Cancer Biother Radiopharm*. 2010;25(3):299–308. <https://doi.org/10.1089/cbr.2009.0695>.
29. Seo Y, Gustafson WC, Dannoon SF, et al. Tumor dosimetry using [(124)I]m-iodobenzylguanidine MicroPET/CT for [(131)I]m-iodobenzylguanidine treatment of neuroblastoma in a murine xenograft model. *Mol Imaging Biol*. 2012;14(6):735–42. <https://doi.org/10.1007/s11307-012-0552-4>.
30. Dickson PV, Hamner B, Ng CYC, et al. In vivo bioluminescence imaging for early detection and monitoring of disease progression in a murine model of neuroblastoma. *J Pediatr Surg*. 2007;42(7):1172–9. <https://doi.org/10.1016/j.jpedsurg.2007.02.027>.
31. Liu X, Li Z, Song Y, et al. AURKA induces EMT by regulating histone modification through Wnt/ β -catenin and PI3K/Akt signaling pathway in gastric cancer. *Oncotarget*. 2016;7(22):33152–64. <https://doi.org/10.18632/oncotarget.8888>.
32. Zhang K, Wang T, Zhou H, et al. A novel Aurora-A inhibitor (MLN8237) synergistically enhances the antitumor activity of sorafenib in hepatocellular carcinoma. *Mol Ther Nucleic Acids*. 2018;13:176–88. <https://doi.org/10.1016/j.omtn.2018.08.014>.
33. Akutagawa J, Huang TQ, Epstein I, et al. Targeting the PI3K/Akt pathway in murine MDS/MPN driven by hyperactive Ras. *Leukemia*. 2016;30(6):1335–43. <https://doi.org/10.1038/leu.2016.14>.
34. Lee C-L, Wahnische H, Sayre GA, et al. Radiation dose estimation using preclinical imaging with 124I-metaiodobenzylguanidine (MIBG) PET. *Med Phys*. 2010;37(9):4861–7. <https://doi.org/10.1118/1.3480965>.
35. Jeff Hirst AKG. AURKA inhibition mimics BRCA1/2. *Aging (Albany NY)*. 2017;9(9):1945–6. <https://doi.org/10.18632/aging.101291>.

Publisher's Note

Springer Nature remains neutral with regard to jurisdictional claims in published maps and institutional affiliations.